Hindawi
Shock and Vibration
Volume 2023, Article ID 6273983, 14 pages
https://doi.org/10.1155/2023/6273983

Research Article

Electrohydraulic Servo Shaker Control Based on the Single Layer Flexible Structure Load

Tao Wang[1] **and Jinchun Song**[2]

[1]*School of Mechanical Engineering, Shenyang Ligong University, Shenyang 110159, Liaoning, China*
[2]*School of Mechanical Engineering and Automation, Northeastern University, Shenyang 110819, Liaoning, China*

Correspondence should be addressed to Tao Wang; molili94@126.com

Received 6 May 2023; Revised 2 June 2023; Accepted 8 June 2023; Published 5 July 2023

Academic Editor: Rodrigo Nicoletti

As a kind of equipment commonly applied in laboratory vibration test simulation, the shaker has been widely used in many important fields of scientific research on experimental engineering vibration. It is employed for the numerical simulation of seismic activities of large buildings to quickly and quantitatively detect and calculate building components related to different building forces, analyze and study various changes of on-site structural forms and the influence mechanism of common earthquake damages or deformations with the actual existence of large-scale seismic activities, as well as to test the antiseismic strengthening structure of buildings to reduce the impact of destructive earthquakes on buildings losses. In general, the load of the shaker is regarded as a rigid structure. But in terms of the load of an electrohydraulic servo shaker with a flexible structure, the system control tends to be nonlinear accompanied by the output signals distorted. In order to achieve the goal of improving the waveform accuracy of shaking tables, it is necessary to combine the corresponding control algorithm strategy. Hence, in compliance with the working principles and functions of shaking table systems, the reasons for the coupling between flexible structure loads and shaking tables are carefully analyzed in this paper. Meanwhile, a control strategy based on the Luenberger observer control method is proposed to effectively realize the coupling suppression within the system and make the output signals of the shaking table reach the required accuracy. Finally, by comparing the frequency characteristic curves of the system before and after the introduction of the Luenberger observer, as well as the output and input analog signals, it can be seen that the Luenberger observer can effectively suppress the impact of oscillations within the system and reproduce the accuracy of the input signals.

1. Introduction

The products and equipment produced in various industries have been working in various extremely complex and harsh real-vibration working conditions for a long time, which more or less affects the performance, quality, and operation safety of these products and equipment systems. For this reason, it is of great necessity to regularly track, research, test, and optimize the actual vibration environment of the products for safer and more reliable operation test results. The main purpose of the shaking table test is to reproduce the real working environment conditions on a regular basis according to the vibration requirements under different working conditions. Therefore, it is more and more extensively applied in plenty of complex engineering fields such as ships, aerospace, road and bridge structures, and rail transit, in which it performs a significant function in the research on the industrial safety development of various countries [1–4].

A shaking table can play an important supporting role in the whole mechanical engineering field. In industrial product systems, if parts are frequently used under the influence of long-term high-frequency vibrations and a series of severe vibration effects such as installation environmental conditions, the reliability is often greatly reduced, and some equipment systems may even be damaged or become invalid eventually. Therefore, with the aim to further fully understand the various operating behavioral

characteristics, reliability, expected working life cycles, and other behavioral characteristics that may occur in a variety of working environments with complex vibrations, it is crucial to conduct a numerical simulation for the characteristics of such working environments with various complex vibrations [5–8].

The design of the drive system of an electrohydraulic servo shaker possesses some remarkable advantages, such as a high thrust power, a faster response to vibration, and a strong ability to bear various loads, which can ensure the realization of more accurate and realistic vibration simulations. Consequently, there has been an increasing in-depth theoretical research on the theory of electrohydraulic servo shaking tables, which has been a more and more in-depth theoretical research, and has been applied to various simulated environments with vibrations [9, 10]. However, when considering the load characteristics of various types of structures, especially under the premise of many practical applications such as the flexible structure of test pieces, some factors like complex coupling are inevitable in the characteristics of flexible structure loads and overall servo shaking tables, while the severity directly affects the control efficiency and accuracy. Moreover, due to the influence of diversified complex reality and nonlinear factors on the overall system of a servo shaking table, the overall control strategy often leads to difficulties in achieving an accurate and reliable control. Apart from that, the entire electrohydraulic shaking table system still has problems such as a difficult waveform reproduction and a low accuracy [11, 12].

The test control system of a shaker is required to have the characteristic of an accurate, efficient, and high-precision waveform reproduction. However, there is always a coupling effect among the load of some flexible structures and a shaker, which seriously restricts the test control and accuracy of signals of the overall shaking table system [11, 13, 14]. In the case that the coupling effect still exists at present, it is not significant to continue other signal quality control analyses in the system. Therefore, in order to ensure the final realization of a high-precision, reliable, and stable waveform output of the system, the key is to minimize the impact of its coupling [15–17]. Underwood and Keller expressed the internal force in the coupling system by introducing two degrees of freedom, making the force generated by coupling based on these two degrees of freedom equal to zero to achieve the main goal of the coupling system control theory [18]. In view of the importance of the mechanism with stiffness (and damping) parameter characteristics, Hayward et al. deduced a specific kinematic design for the decoupling controller of an architecture device [19]. Filabi and Yaghoobi proposed a trajectory fuzzy adaptive sliding mode decoupling controller in a Cartesian space coordinate system which consisted of sliding mode control and an adaptive learning algorithm, thus ensuring the closed-loop stability and finite time convergence of tracking errors without relying on any parameter initialization condition [20]. Yang constructed a continuous integral robust control algorithm with an asymptotic tracking performance and an adaptive learning algorithm based on neural networks for constrained nonlinear systems to deal with high-order uncertain nonlinear systems with disturbances [21, 22].

Plummer designed a multivariable controller for coupling the multichannel servo system which was the allowed channel to be decoupled from the individually-assigned pole position, which was applied to the dual-channel electrohydraulic servo system [23]. In order to reduce the position synchronization error caused by different dynamics, Jeonga and You designed acceleration and speed controllers based on the proportional integral (PI) control law, and the coupling of each axis was reduced by comparing the maximum error [24]. Chen proposed a new structure of cross-coupled position command shaping controller (CPCSC) for precise tracking during multiaxis motion control. Compared with the traditional multiaxis cross-coupled control (CCC) system, this new structure had a simpler design process and a better stability than the traditional compensator [25]. Adam studied an experiment on a small-scale primary secondary flexible load structure excited by an earthquake, where the secondary structure attached to the elastic-plastic shear frame was tested with and without conditions. In the numerical study, the mechanical model of the structure under study was excited by the digitally-recorded acceleration base, and the flexible nonlinear force displacement relationship could be measured [26]. Cao and Khan evaluated the behavior and performance of multiscale hybrid composite materials under seismic loads using a single degree of freedom hydraulic shaker [27]. A shaking table test of a two-story steel frame was introduced under simulated seismic loads, which could display second-order inelastic behavior and avoid lateral torsional buckling of individual components [28].

Although many scholars have conducted research on this issue, there are still some limitations. First, although there are many studies on vibration suppression based on mechanical platforms, for example, robust algorithms, adaptive algorithms, and neural network algorithms, there is not much research on the load of electrohydraulic servo shaking tables. So, the research based on the electrohydraulic servo shaking table platform has exposed certain research deficiencies. Second, the other research topic mainly focuses on symmetrically distributed actuators, considering fewer asymmetric actuator components. The electrohydraulic servo shaker based on a flexible structural load often leads to large coupling in the system and affects its control performance. Within the required bandwidth range of a system, the oscillations that form resonance and antiresonance peaks exceed the stable range of its system amplitude [29, 30].

The Luenberg observer-based method proposed in the 1970s is a robust control method for the linear system. The basic idea is to control the input, observer, and output error variables of the system so that the estimation error tends to zero, so as to suppress the oscillation in the system and achieve the effect of signal tracking, which is a very useful method in the hydraulic servo system. To further improve the waveform reproduction method of the hydraulic servo shaker control system, this paper proposes a decoupling control method relying on the Luenberger observer to address common issues such as the coupling between the

shaking table and the flexible structural load, so as to enhance the overall dynamic tracking performance of the shaker. The specific content of the article is as follows:

(1) In order to study the dynamic performance of an electrohydraulic servo shaking table based on flexible loads, a mathematical model of the asymmetric hydraulic cylinder of its hydraulic servo is constructed, and a simplified diagram and model of the flexible structural load are established.

(2) By introducing and analyzing the three-state control strategy commonly used for electrohydraulic servo shaking tables, the mathematical transfer function of the system is established, with the limitations of its application illustrated, which lays the foundation for the introduction of observer methods in the future.

(3) With the introduction of the control algorithm of the Luenberger observer, its application to the study of electrohydraulic servo systems and the method of adjusting its internal parameters are both explained.

(4) The Luenberger observer is adopted into the system since the aforementioned three-state control strategy is not sufficient to suppress the oscillation effect of flexible loads according to the comparative analysis of examples. The comparison results show that the observer can significantly suppress the impact of within the system and achieve the function of reproducing the input signals.

2. Electrohydraulic Servo Shaker

2.1. Modeling of the Electrohydraulic Servo System. A hydraulic servo drive control system mainly includes a power control system, an electrohydraulic servo valve, a hydraulic cylinder, a sensor circuit, signals, and a conditioning device module structure. In order to better facilitate the computer simulation performance analysis and system modeling, it is necessary to establish a dynamics and simulation mathematical model of the hydraulic drive excitation system and describe the system and explain the dynamics characteristics for the basic components of each subsystem as well as their relationships. The relationship between the parameters and variables of system characteristics described through the dynamic model analysis method is often the law of continuous changes of dynamics with unit time.

In order to systematically analyze the load of a hydraulic shaking table, it is necessary to establish a mathematical model based on an electrohydraulic servo system and analyze its dynamic characteristics. A typical asymmetric hydraulic cylinder-valve control model is established in this section, which is then reasonably simplified. Based on the system data required by simulation calculation, a more reasonable and complete mathematical model is established for the hydraulic servo shaking table.

The basic form of the ideal asymmetric hydraulic cylinder is shown in Figure 1. We set the movement to the right as the positive direction and vice versa as the negative direction. According to the selected ratio, $n = A_2/A_1$; so, the flow relationship is as follows:

$$q_2 = nq_1, \tag{1}$$

where q1 is the flow rate of the rodless chamber into the asymmetric hydraulic cylinder (L/min); q2 is the flow rate of the rod chamber flowing out of the asymmetric hydraulic cylinder (L/min); A1 is the flow rate of the rodless chamber (m3); and A2 is the flow rate of the rod chamber (m3).

The spool valve flow equation, the hydraulic cylinder continuous equation, and the force balance equation are the three basic equations of the servo valve-controlled hydraulic cylinder system. The following formula describes the dynamic performance of the valve-controlled asymmetric hydraulic cylinder [12, 31].

$$\begin{aligned} q_L &= K_q x_v - K_c p_L, \\ q_L &= C_{tc} p_L + \frac{1+n^2}{1+n^3}\frac{V_e}{\beta_e}\frac{\mathrm{d}p_L}{\mathrm{d}t} + \left(\frac{A_1+A_2}{2}\right)\frac{\mathrm{d}y}{\mathrm{d}t}, \\ A_1 p_1 - A_1 p_1 - A_2 p_2 &= m\frac{\mathrm{d}^2 y_p}{\mathrm{d}t^2} + B\frac{\mathrm{d}y}{\mathrm{d}t} + Ky. \end{aligned} \tag{2}$$

After obtaining the transfer function through the mathematical modeling of the asymmetric hydraulic cylinder, the positive motion transfer function shown below can be obtained after Laplace transformation.

$$\frac{Y}{X_v} = \frac{K_q/A_1}{mV_t/4\beta_e A_1^2 s^3 + \left(1 + n^3/1 + n^2 mK_{ce}/A_1^2 + BV_t/4\beta_e A_1^2\right)s^2 + \left(1 + n^3/1 + n^2 BK_{ce}/A_1^2 + KV_t/4\beta_e A_1^2 + 1 + n/2\right)s + 1 + n^3/1 + n^2 KK_{ce}/A_1^2}, \tag{3}$$

where K_q is the flow gain (m); x_v is the spool displacement (m); V_t is the equivalent volume (m^3); B is the viscous damping coefficient (N·s/m^2); β_e is the bulk elastic modulus of hydraulic oil (Pa); K_{ce} is the system leakage coefficient (m^5/(N·s)); K is the system load stiffness (N/m); and m is the load mass, (m^2/s).

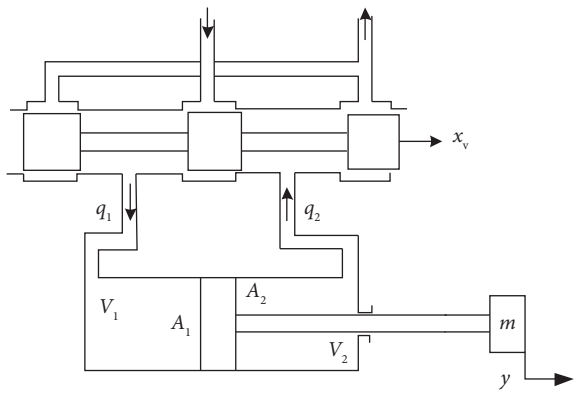

Figure 1: The model of the asymmetric cylinder system with flexible connection.

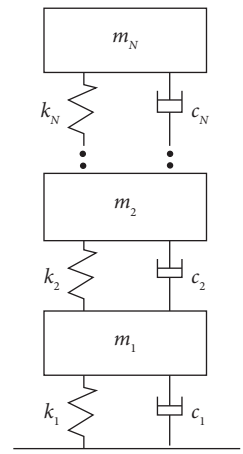

Figure 2: Flexible structure specimen model.

Similarly, the three equations of negative motion can be obtained, and the transfer function formula of negative motion is as follows:

$$\frac{Y}{X_V} = \frac{K_q/\mathrm{A}}{1 + n^2/n\left(1+n^3\right)mV_t'/4\beta_e A_1^2 s^3 + \left(1/nmK_{ce}^{'}/A_1^2 + 1 + n^2/n\left(1+n^3\right)BV_t'/4\beta_e A_1^2\right)s^2 + \left(1/nBK_{ce}^{'}/A_1^2 + 1 + n^2/1 + n^3 KV_t'/4\beta_e A_1^2 + 1 + n/2\right)s + 1/nK_{ce}^{'}/A_1^2}. \tag{4}$$

2.2. Mechanical Model of the Flexible Specimen. The modal analysis of the force on the flexible test piece is carried out through vibration. The mechanical analysis of the flexible test piece installed and fixed on the shaking table is as shown in Figure 2, and its mechanical motion equation expression is as follows:

$$m_p s^2 x + c_p s x' + k_p x' = 0, \tag{5}$$

where x is the absolute displacement of each particle. x' is the relative displacement of each particle. m_p, c_p, and k_p are the mass matrix, damping matrix, and stiffness matrix of the specimen, respectively.

As shown in Figure 3, the entire framework is divided into a top-level structure and a bottom-level structure, as shown below.

$$m_2\ddot{x}_2 + c_2\dot{x}_2 + k_2 x_2 = -m_2\ddot{u}_g + T, \tag{6}$$

where, $\ddot{x}$, $\dot{x}$, and x express the acceleration, velocity, and displacement. $\ddot{u}_g$ represents the ground acceleration. T is the shear force between members. Theoretically, the shear force can be derived from the force feedback minus the inertial force of the rigid table. However, the sample mass used in this test is not too big and difficult to identify and differentiate from force feedback; so, this paper adopts the neglect treatment.

According to the modal knowledge, the acceleration of the flexible structure sample fixed on the vibration test bench is calculated, namely, the apparent mass as follows:

$$\begin{aligned}\overline{M}(s) &= \frac{F(s)}{A(s)} \\ &= I^T m_p\left[I - \sum_{n=1}^{N}\varphi_n \frac{\varphi_n^T m_p I s^2}{M_n\left(s^2 + 2\zeta_n\omega_n s + \omega_n^2\right)}\right],\end{aligned} \tag{7}$$

where $\varphi_n = (\varphi_{n1}, \varphi_{n2}, \cdots, \varphi_{nN})^T$ is the mode shape vector of the nth order. M_n is the nth order formation mass, ω_n is the nth order formation natural frequency, and ζ_n is the nth order formation damping ratio.

The apparent mass can be further decomposed into the sum of several single-degree-of-freedom systems, namely,

$$\overline{M}(s) = \sum_{n=1}^{N} m_{en}\frac{2\zeta_{en}\omega_n s + \omega_n^2}{s^2 + 2\zeta_{en}\omega_n s + \omega_n^2}, \tag{8}$$

where m_{en} is the nth-order equivalent modal mass and ζ_{en} is the nth-order equivalent modal damping ratio of the simplified system.

Generally, the vibration stiffness of a load table structure system is relatively large, which can be simply regarded as a vibration rigid body. The amount of flexibility and deformation that can directly causes vibration due to vibration stiffness in the motion state is correspondingly small. As a result, in some cases with a proper design and control, the influence on the local vibration deformation of a shaking table system itself is very small or even negligible. However, if frame-type members are directly composed of flexible structural forms such as a bottom plate and a roof beam, the

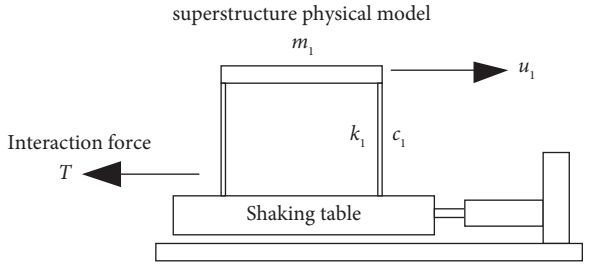

Figure 3: Sketch-map of problem prototype: the hydraulic servo shaking table based on flexible structural load.

rigidity of this flexible structure is extremely limited, and it cannot be simply approximated as a rigid structure. Additionally, in terms of designing the control algorithm of a shaking table, it is essential to consider the coupling between the shaker and the load and suppress the oscillations caused by the deformation of structural parts during operation.

3. Three-State Control Strategy

For a shaking table system driven through the acceleration signal control method, in order to satisfy the requirements of improving the accuracy of output signal and the response frequency, one or more strategy control methods that can be optimized need to be adopted on the shaking table. In order to quickly and accurately obtain the expected system acceleration signal of the system, it is necessary to perform corresponding algorithms and analyses on the reference acceleration signal and feedback acceleration signal during the actual measurement through a control system environment analysis. Three-state control is a classical control strategy algorithm based on the shaking table. Figure 4 shows the system block diagram of the three-state control strategy. K_{dr}, K_{vr}, and K_{ar} represent the three-state feedforward control parameters of the algorithm, and K_{df}, K_{vf}, and K_{af} represent the three-state feedback control parameters of the algorithm. $y_d\ (k)$ represents the acceleration feedback signal, and $x_d\ (k)$ represents the corresponding reference signal. The gains of the P controller are K_d, K_v, and K_a. K_c is the total gain [32–34].

In order to complete the design requirements of the three-state controller, it is necessary to determine the values of the feedforward control K_{dr}, K_{vr}, and K_{ar} parameters and the feedback control K_{df}, K_{vf}, and K_{af} parameters, respectively, and the former is determined by the latter. The open-loop transfer function can be defined as follows:

$$W(s) = \frac{1}{(s/\omega_r + 1)\left(s^2/\omega_{nc}^2 + 2\xi_{nc}/\omega_{nc} + 1\right)}, \tag{9}$$

where ω_r is the frequency corresponding to the acceleration response bandwidth, rad/s. ω_{nc} is generally 1.05~1.20 times the hydraulic natural frequency, rad/s. ξ_{nc} generally takes a value of 0.7.

According to the block diagram in Figure 4, the closed-loop transfer function of the feedback is obtained as follows:

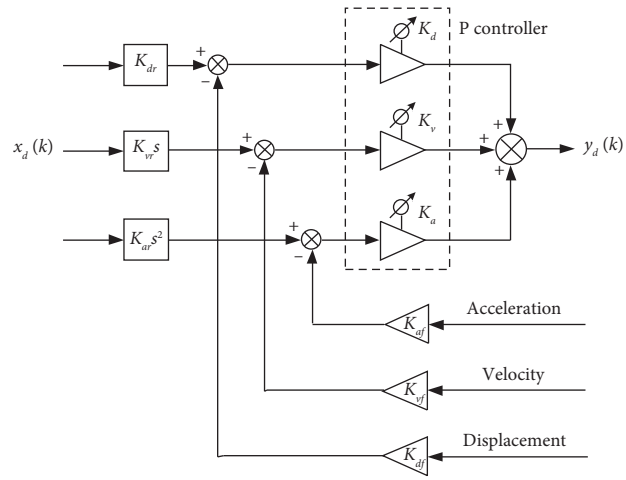

Figure 4: Block diagram of a three-state controller.

$$G_c(s) = \frac{Y_d}{R_d} = \frac{K_{df}K_v}{s^3/\omega_n^2 + \left(K_{af}K_v + 2\xi_n/\omega_n\right)s^2 + \left(K_{vf}K_v + 1\right)s + K_{df}K_v}. \tag{10}$$

Equating the above two formulas, the three parameters of the three-state feedback are as follows:

$$\begin{cases} K_{df} = \dfrac{\omega_r\omega_{nc}^2}{K_v\omega_n}, \\ K_{vf} = K_{df}\left(\dfrac{2\xi_{nc}}{\omega_{nc}} + \dfrac{1}{\omega_r}\right) - \dfrac{1}{K_v}, \\ K_{af} = K_{af}\left(\dfrac{2\xi_{nc}}{\omega_r\omega_{nc}} + \dfrac{1}{\omega_{nc}^2}\right) - \dfrac{2\xi_n}{K_v\omega_n}. \end{cases} \tag{11}$$

The transfer function of the three-state feedforward can be obtained as follows:

$$B(s) = K_{dr}\left(1 + \frac{K_{vr}}{K_{dr}}s + \frac{K_{ar}}{K_{dr}}s^2\right). \tag{12}$$

Taking $K_{dr} = K_{df}$, the three parameter expressions of the three-state feedforward are obtained as follows:

$$\begin{cases} K_{vr} = K_{df}\dfrac{2\xi_{nc}}{\omega_{nc}}, \\ K_{dr} = K_{df}, \\ K_{ar} = \dfrac{K_{df}}{\omega_{nc}^2}. \end{cases} \tag{13}$$

The basic control technology principle of three-state servo control widely used in the technologies is discussed through a comprehensive and systematic analysis.

Given some inherent shortcomings of the hydraulic system control itself such as relatively small damping and a narrow frequency width of system signal response frequency, a basic control technology using pole configuration is adopted to redesign the three-state servo hydraulic system method. Besides, a feedback filter is utilized to improve the damping characteristics of the system, and a feedforward filter is employed to eliminate the interference characteristics of the neutral pole generated due to the frequency response damping characteristics of the system, so as to realize the improved frequency response characteristics of the system.

4. Luenberger Observer

4.1. The Equipment Principle of the Luenberger Observer. The Luenberger observer theory which was first proposed by Luenberger, Kalman, and Busey et al. is specially designed to solve the dynamic control problems of more complex systems. When the state quantity of some dynamic complex systems is difficult to obtain through an accurate quantification, a more accurate system state quantity is often required. By changing the input and output of a complex system to reconstruct state variables, it is possible to finally obtain state variables that are relatively easily calculated via computers, which may be the target of the Luenberger observer design. The Luenberger observer is designed and established through a system model, whose positive input and inverse output can be directly regarded as the input of the Luenberger observer system. To obtain the feedback value of the control system, it is necessary to make a difference between the actual observation value needs to be estimated, and the poles of the system are configured on this basis [35–37].

We set the system model as follows:

$$\begin{cases} \dot{x} = \mathbf{A}x + \mathbf{B}u, \\ y = \mathbf{C}x, \end{cases} \tag{14}$$

where x is the state variable; u is input; y is the output; $\mathbf{A}$ is the state matrix; $\mathbf{B}$ is the input matrix; and $\mathbf{C}$ is the output matrix.

In order to construct the Luenberger observer, it is necessary to input the feedback matrix into the state equation. The block diagram of the structural model is shown in Figure 5. As shown in the following formula, the Luenberger observer is formed by adding the error between the estimated value of the observer and the estimated value of the system.

$$\begin{cases} \dot{\hat{x}} = \mathbf{A}\hat{x} + \mathbf{B}u + \mathbf{H}(y - \hat{y}), \\ \hat{y} = \mathbf{C}x. \end{cases} \tag{15}$$

We define the real state variables of the system and the error of the observer's estimated state as follows:

$$e = x - \hat{x}. \tag{16}$$

The pole in the matrix (A−HC) determines whether the error of the system state estimation can be attenuated to zero. We substitute the above formula to get [38]

$$\begin{aligned} \dot{e} &= \dot{x} - \dot{\hat{x}} \\ &= \mathbf{A}x + \mathbf{B}u - \mathbf{A}\hat{x} - \mathbf{H}(y - \hat{y}) - \mathbf{B}u \\ &= \mathbf{A}(x - \hat{x}) - \mathbf{HC}(x - \hat{x}) \\ &= (\mathbf{A} - \mathbf{HC})(x - \hat{x}) \\ &= (\mathbf{A} - \mathbf{HC})e. \end{aligned} \tag{17}$$

As the known system characteristic $\mathbf{A}$ and matrix $\mathbf{C}$ have been determined by the system characteristics, whether the estimated error of the system state can be completely attenuated to zero or not, the main factor lies in the feedback matrix coefficient $\mathbf{H}$. Therefore, designing and adjusting the feedback matrix can effectively make the state estimation error of the whole system have a good decay rate.

For the disturbance term of equation, the Lyapunov function is constructed as follows:

$$V = \frac{1}{2}e^2. \tag{18}$$

Taking the derivation of the Lyapunov function of formula, the following can be obtained.

$$\begin{aligned} \dot{V} &= e\dot{e} \\ &= e(\mathbf{A} - \mathbf{HC})e \\ &= (\mathbf{A} - \mathbf{HC})e^2. \end{aligned} \tag{19}$$

If the eigenvalue of (A−HC) can be kept negative, the relationship is as follows:

$$\begin{cases} V \longrightarrow 0, \\ e \longrightarrow 0. \end{cases} \tag{20}$$

Therefore, in order to make the error of the system converge and make it operate stably, it is necessary to take the appropriate value of H to make the corresponding matrix ($\mathbf{A}$−HC) eigenvalue negative.

4.2. Design of the Luenberger Observer for the Hydraulic System. The observer-based suppression method is a simple and easy-to-implement approach that involves introducing acceleration feedback control. Theoretically, this method can enhance the active damping of the system, leading to the suppression of the acceleration feedback. Figure 6 represents a simplified block diagram of the load disturbance observer.

The transfer function of this observer is as follows:

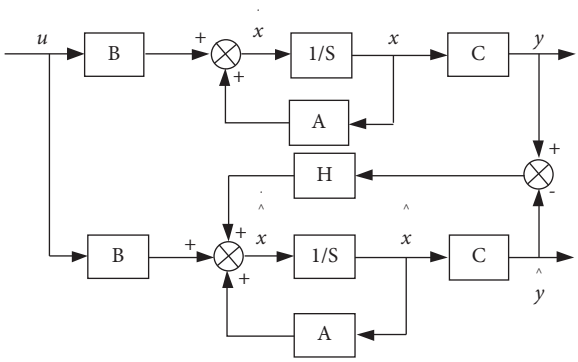

Figure 5: Structure of the Luenberger state observer.

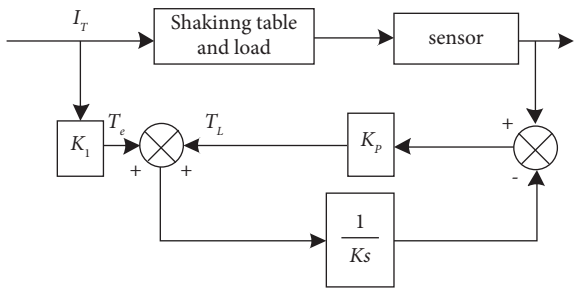

Figure 6: Structure diagram of a simplified load disturbance observer.

$$\frac{T_L}{T_e} = \frac{1}{K/K_p s + 1}. \tag{21}$$

As per the formula provided above, it can be observed that it behaves like a low-pass filter, which indicates there is no need to pay more attention to stability concerns. Moreover, the relationship between its parameters and the resonant point frequency can be represented by the equation:

$$\frac{K_p}{K} = \omega^2. \tag{22}$$

Figure 7 illustrates the construction of a Luenberger observer that requires double integration of position observation values. An error value is then derived by subtracting the measured value from the observed one. Finally, a PID control regulator is employed to drive the error value towards zero.

The transfer function of this observer is as follows:

$$P_{est} = I_T \frac{s^2}{s^3 + K_D s^2 + K_p + K_I} + T_M \frac{K_D s^2 + K_p + K_I}{K_D s^2 + K_p + K_I}. \tag{23}$$

According to the characteristics of the electrohydraulic servo shaking table, once the structure of the executing components of the vibration table and parameters of its flexible load are determined, the resonance value within the system is also confirmed. By using

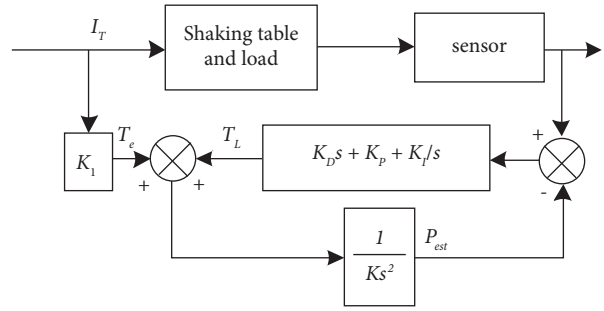

Figure 7: Structure of the Luenberger observer for load disturbance.

Figure 8: Schematic diagram of equipment.

the sinusoidal scanning method, the frequency value of the oscillation point, which is the value of ω, can be determined. As a consequence, according to formula (22), the size of K can be naturally obtained after a specific value of K_P is chosen based on PID control rules. Then, the selected value can be input into the simulation system of the Luenberger observer to check the effectiveness of suppressing oscillations and determine if any relevant parameters need to be adjusted.

5. Case Analysis

As described in Figure 8, the mechanical structure of the shaker mainly consists of a vibrating test table, a bracket, a fixed structure, a guiding device, a foundation base, and a connecting mechanism. The force is transmitted to an excited test object through vibration. To guarantee external forces can be borne and transferred to a stressed object, the table top itself should be equipped with relatively good overall strength stability and torsional bending stiffness, whose overall production material is required to be lightweight as far as possible. For the sake of maximizing the impact of the high-frequency natural vibration of the table top on the overall phenomenon, the natural vibration frequency should not be distributed within the operating frequency. Notably, the smaller the mass proportion of the worktop is, the greater the performance is.

The main components of a hydraulic power system include a booster pump station, a servo valve, a servo cylinder, an overflow valve, as well as various pressure and temperature instruments. A pump station is usually composed of a main oil source, an axial piston variable displacement pump, a motor, a hydraulic overflow valve, and other components. An overflow valve can be used to

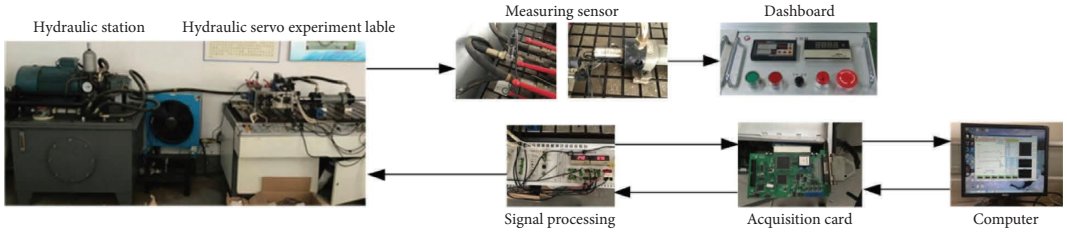

Figure 9: Control system of an electrohydraulic servo shaking table.

Table 1: Hydraulic system parameter values.

Parameter names	Parameter symbols	Units	Parameter values
Flow gain	K_q	m^2/s	1.2
Effective bulk modulus of elasticity	β_e	MPa	690
Stiffness of hydraulic spring	K_h	N/m	7.91×10^6
	K_h'	N/m	4.45×10^6
Total flow pressure	K_{ce}	$m^5/(N \cdot s)$	10.9×10^{-13}
	K_{ce}'	$m^5/(N \cdot s)$	8.11×10^{-13}

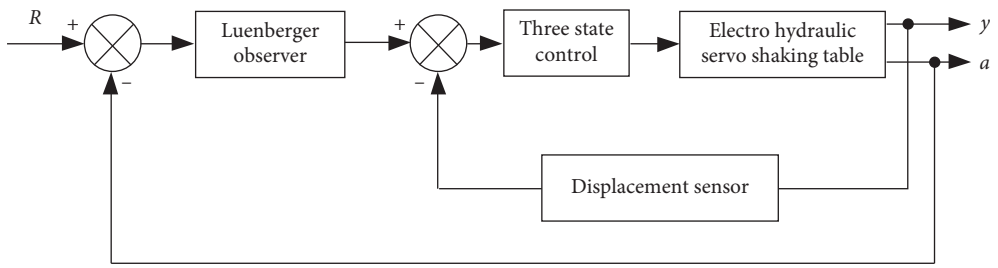

Figure 10: Principle diagram of Luenberger observer coupling suppression of an electrohydraulic servo shaker.

measure and regulate the oil supply pressure of the system, which can effectively and reasonably protect its hydraulic components so that the maximum pump inlet pressure cannot exceed the maximum usable pump outlet pressure. It can also be ensured that the automatic overflow function of the system can be realized when the filter is blocked and an alarm signal is sent, so as to protect the components of the hydraulic servo system from being contaminated by impurities. A pressure instrument is mainly used for real-time monitoring of the actual differential pressure changes in the oil cylinder of the servo system and the actual back pressure of the servo valve system online, so as to accurately analyze the normal working movement process and pressure state. A filter can be applied to efficiently filter the fine particles and impurities left in the oil pipelines to satisfy the requirements of a normal and safe use of servo pump valves [39, 40].

The control system of an electrohydraulic servo shaker is presented in Figure 9. A system control unit mainly consists of an electrohydraulic servo valve, a data acquisition card, signal conditioning devices, and various sensors. The controller sends signals directly to the amplifier of the servo valve, and the system directly converts the input voltage signals of low energy into high-power signals. The hydraulic cylinder outputs the corresponding vibration waveform to excite the object to be measured, and the displacement sensor built in the hydraulic cylinder as well as the acceleration sensor of the system to be tested are fed back to the controller. Eventually, continuous corrections are accomplished through the controller according to the error information between the feedback drive system signals and the feedback system signals [41–43].

In the electrohydraulic servo control system, the hydraulic actuator ensures fast response and load, and the electrical components provide the convenience and flexibility of the system. The use of circuit control can provide high rapidity and ensure large output force and power. The specific parameter values are shown in Table 1.

The schematic diagram of the coupling vibration suppression of the flexible structural load of the electrohydraulic servo shaker is shown in Figure 10. Compared with the rigid load, more obvious frequency fluctuations are produced at the antiresonance through a control system with a flexible connection load. On the basis of the three-state control of the shaking table, the internal of the system can be improved after adding a Luenberger observer to the loop. In the presence of a high damping coefficient, the impact of such oscillations can be effectively reduced while having little impact on the system itself. The frequency should be as close to the peak frequency of the oscillations as possible, so as to reduce the deviation of the suppression frequency.

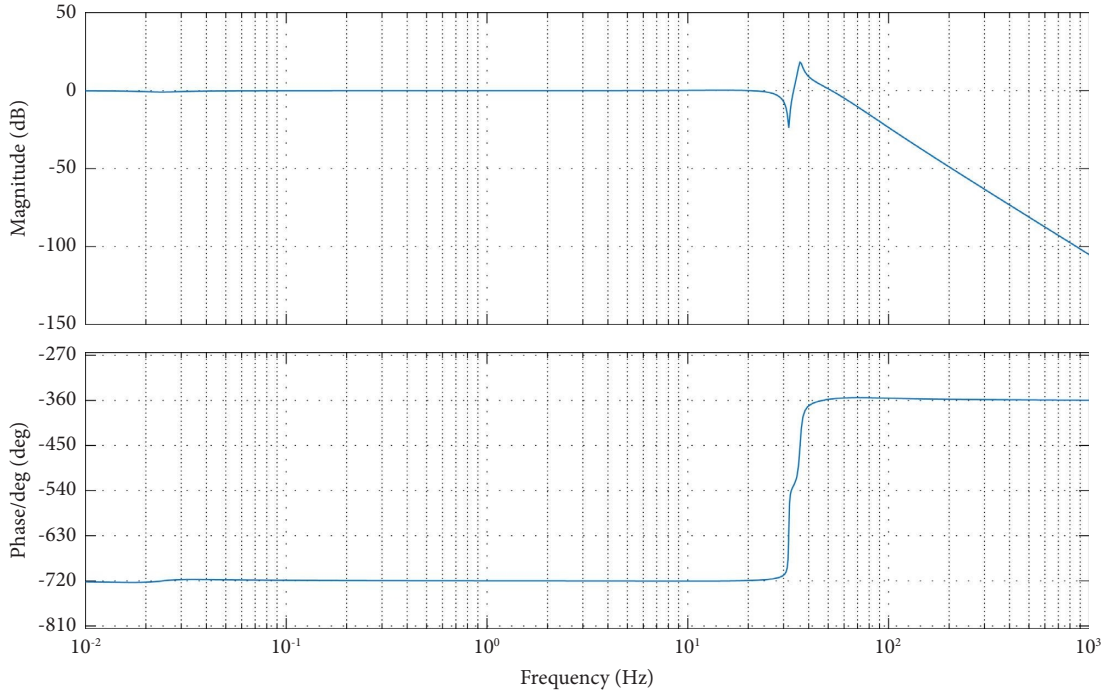

Figure 11: Frequency response of the system without optimize control.

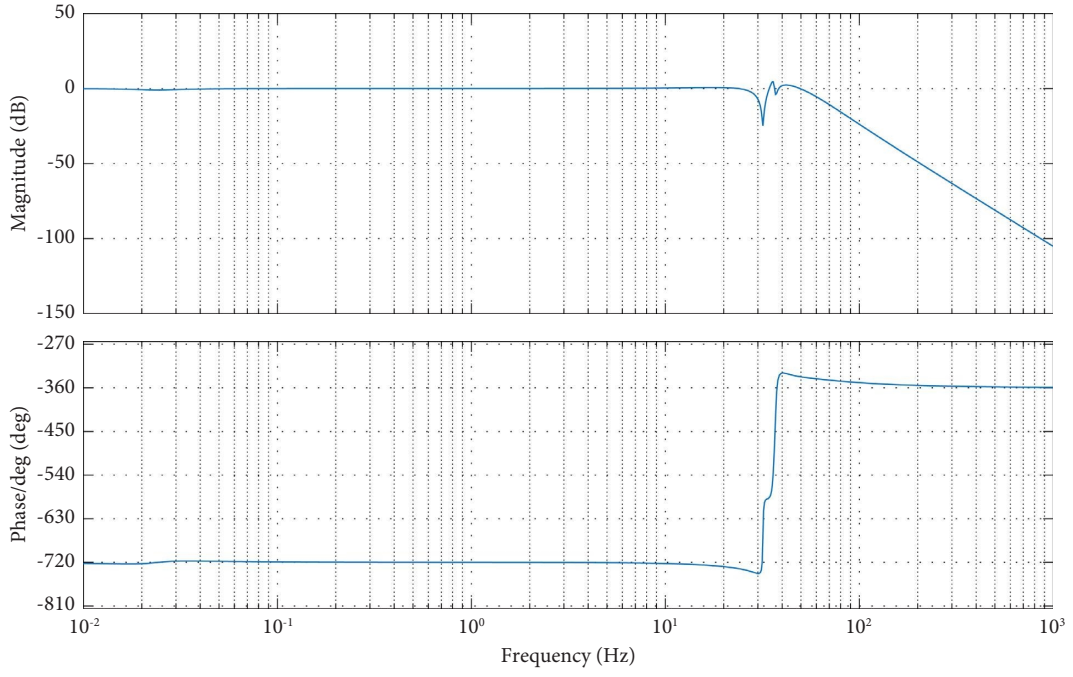

Figure 12: System frequency response with three-state control introduced.

As is shown in Figures 11 and 12, the three-state servo control system is mainly applied to rigid specimens, but most of which are used in practice generally contain flexible structures. When the control theory method is applied to the test work on the flexible frame specimen, it is easy to cause the instability of the whole system state, and it is necessary to consider adding other algorithm controls. The frequency characteristic simulation diagram of the system after suppression through the Luenberger observer is shown in Figure 13. It can be seen that the Luenberger observer can better suppress the oscillation effect, reduce the coupling effect, and enhance the system stability. Figure 14 shows a simulation comparison diagram of the output and input random acceleration signals, from which it can be seen that the input signals can be accurately reproduced with a suppressed acceleration waveform.

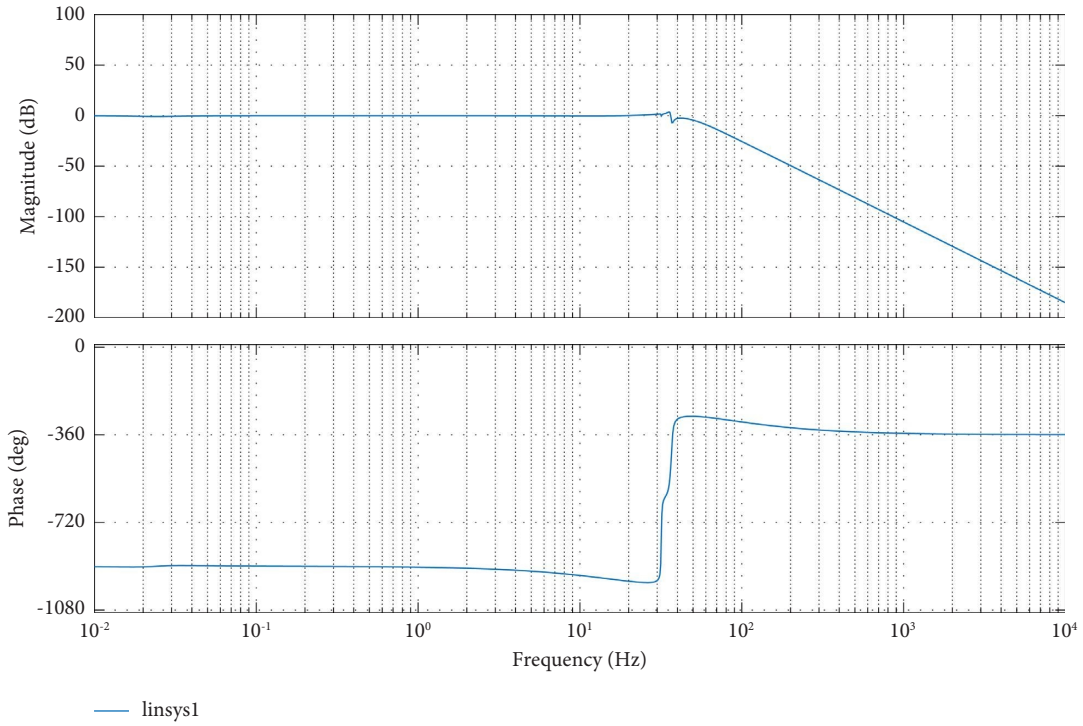

Figure 13: System frequency response with Luenberger observer introduced.

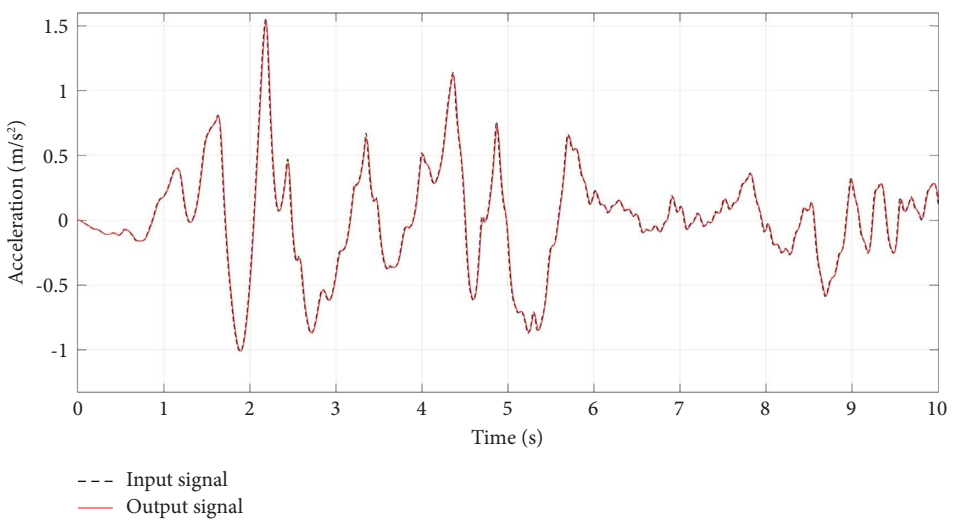

Figure 14: Comparison of output and input acceleration analog signals.

As the load mass increases, the system coupling frequency moves to a low level, as is shown in Figures 15 and 16. The resonance can be restrained through three-state control, but the antiresonance has no obvious effect. The system frequency characteristic simulation diagram after using the Luenberger observer for suppression is shown in Figure 17, from which it can be seen that the Luenberger observer still has a good suppression effect, and that oscillation peaks of the system are suppressed. From the simulation comparison of the output and input acceleration signals in Figure 18, the suppression scheme of the Luenberger observer has better tracking accuracy and can satisfy the requirements of loading acceleration signals.

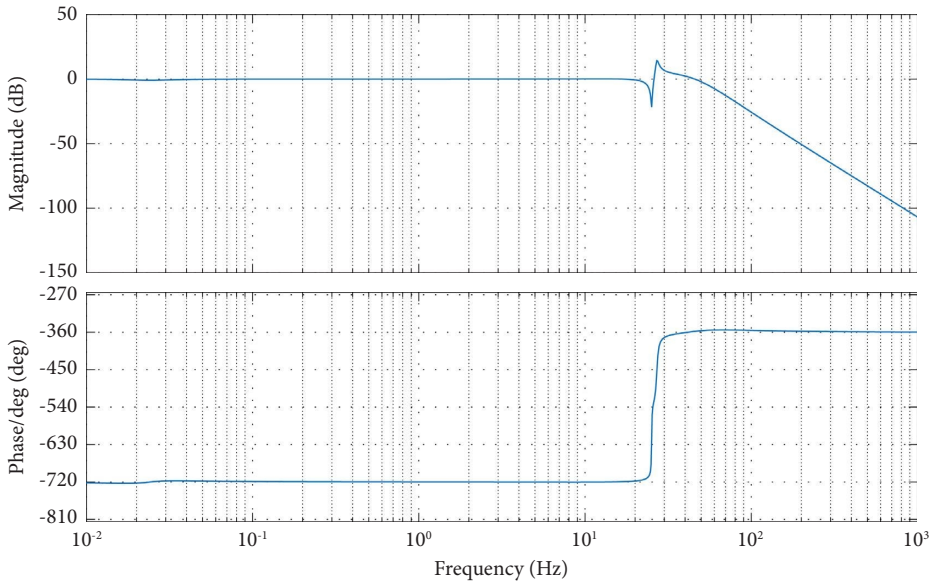

Figure 15: Frequency response of the system without three-state control.

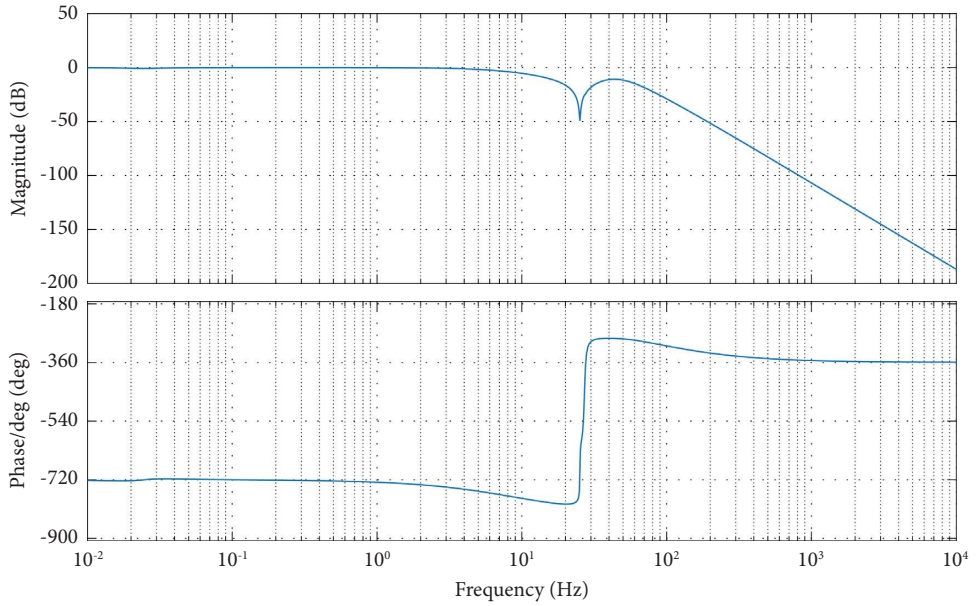

Figure 16: System frequency response with three-state control.

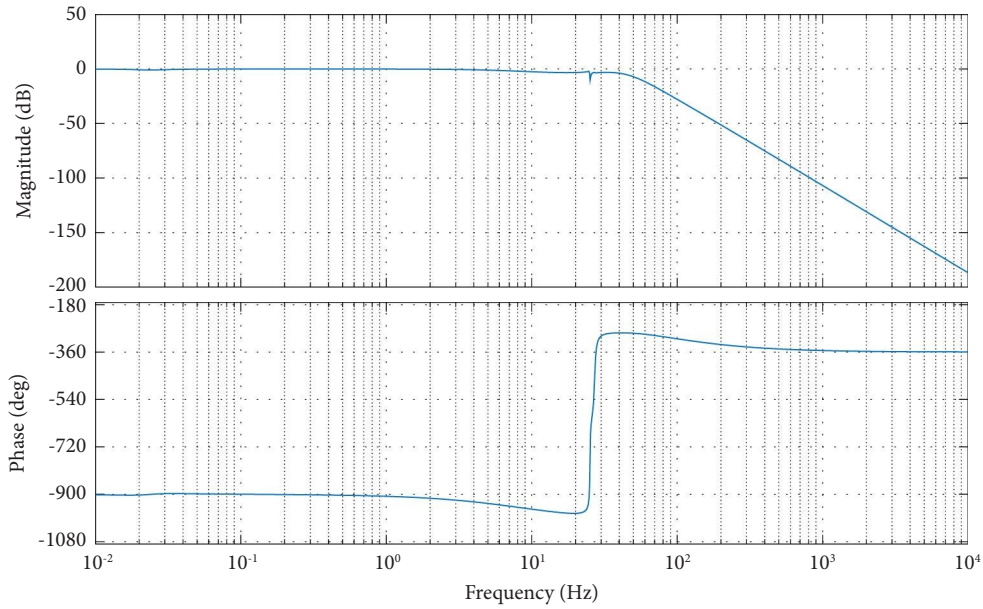

Figure 17: System frequency response with the Luenberger observer.

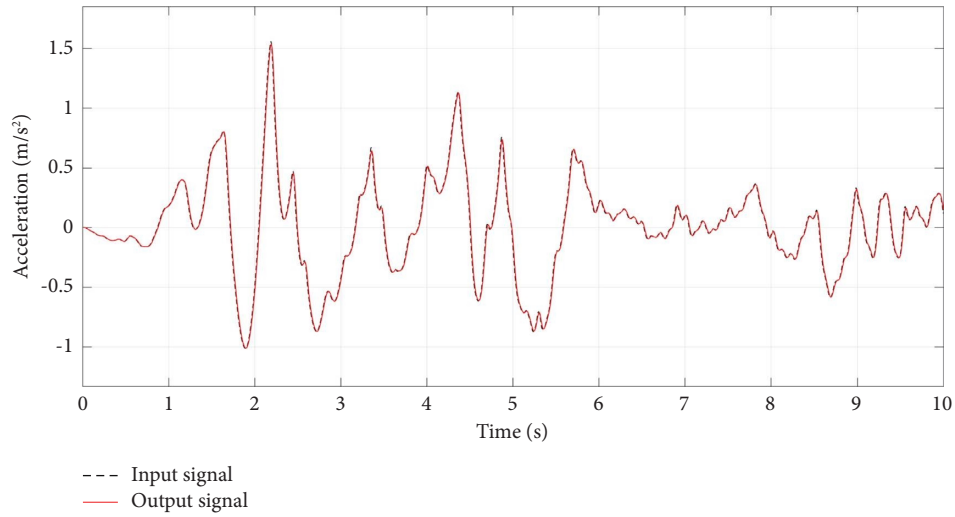

Figure 18: Comparison diagram of output and input acceleration analog signals.

6. Conclusion

Shaking tables are a kind of special test monitoring equipment that can effectively realize the vibration simulation measurement of seismic signals in the industrial experimental environment systems, which can provide a working environment with real vibrations that simulate daily workplaces for various industrial products. However, in practice, an upper platform loaded with a flexible structure easily results in a large coupling output. In view of this, the paper conducts a detailed analysis of the reasons for the coupling between shakers and flexible structural loads and proposes a corresponding suppression control scheme. The mechanical model of a flexible structure specimen system is systematically analyzed based on a shaker. In addition, with the introduction of the related concepts of apparent mass control, the three-state servo control-related parameters set according to the apparent mass controller are used to calibrate the performance of the hydraulic system. Aiming at the shortcomings of the three-state control strategy, the adoption of a Luenberger observer is proposed to suppress system coupling. By observing the frequency characteristic curves of the system, it can be concluded that the influence of oscillations in the system has been eliminated. After comparing the output and input acceleration simulation signals, the input signals can be accurately reproduced, which verifies the effectiveness of the Luenberger observer control method.

Subsequent research can further concentrate on investigating the vibration loads based on multilayer mass flexible structures on this theoretical basis and analyzing the dynamic performance relationship between electrohydraulic

servo shaking tables and loads. It is also hoped to explore the specific applications of higher performance control algorithms in the suppression of oscillation in electrohydraulic shaking tables, such as improving the reproducibility of input waveforms and control accuracy of vibration systems through the nonlinearity of electrohydraulic servo systems, relying on neural networks or robustness methods.

Data Availability

The data used to support the findings of this study are included within the article.

Conflicts of Interest

The authors declare that they have no conflicts of interest.

Acknowledgments

This project was supported by the the scientific research support plan of Shenyang Ligong University to introduce high-level talents (1010147001113).

References

[1] A. R. Plummer, "Control techniques for structural testing: a review," *Proceedings of the Institution of Mechanical Engineers-Part I: Journal of Systems & Control Engineering*, vol. 221, no. 2, pp. 139–169, 2007.

[2] J. H. Jin, H. C. Na, and S. B. Jeon, "Kinematic analysis of multi axis shaking table for multi-purpose test of heavy transport vehicle," *Journal of Institute of Control, Robotics and Systems*, vol. 18, no. 9, pp. 823–829, 2012.

[3] X. Cheng, X. Zhou, H. Liu, Y. C. Zhou, and W. Shi, "Numerical analysis and shaking table test of seismic response of tunnel in a loess soil considering rainfall and traffic load," *Rock Mechanics and Rock Engineering*, vol. 54, no. 3, pp. 1005–1025, 2021.

[4] L. Cao, C. Yang, and J. Zhang, "Derailment behaviors of the train-ballasted track-subgrade system subjected to earthquake using shaking table," *KSCE Journal of Civil Engineering*, vol. 24, no. 10, pp. 2949–2960, 2020.

[5] M. Nakashima, T. Nagae, R. Enokida, and K. Kajiwara, "Experiences, accomplishments, lessons, and challenges of E-defense—tests using world's largest shaking table," *Japan Architectural Review*, vol. 1, no. 1, pp. 4–17, 2018.

[6] J. Cravero, A. Elkady, and D. G. Lignos, "Experimental evaluation and numerical modeling of wide-flange steel columns subjected to constant and variable axial load coupled with lateral drift demands," *Journal of Structural Engineering*, vol. 146, no. 3, pp. 1–19, 2020.

[7] D. Pietrosanti, M. De Angelis, and A. Giaralis, "Experimental study and numerical modeling of nonlinear dynamic response of SDOF system equipped with tuned mass damper inerter (TMDI) tested on shaking table under harmonic excitation," *International Journal of Mechanical Sciences*, vol. 184, no. 184, Article ID 105762, 2020.

[8] D. Song, X. Liu, J. Huang, Y. F. Zhang, J. M. Zhang, and B. N. Nkwenti, "Seismic cumulative failure effects on a reservoir bank slope with a complex geological structure considering plastic deformation characteristics using shaking table tests," *Engineering Geology*, vol. 286, Article ID 106085, 2021.

[9] R. Enokida and K. Kajiwara, "Nonlinear signal-based control for single-axis shake tables supporting nonlinear structural systems," *Structural Control and Health Monitoring*, vol. 26, no. 9, pp. 1–20, 2019.

[10] H. Jordão, A. J. Sousa, and M. T. Carvalho, "Optimization of wet shaking table process using response surface methodology applied to the separation of copper and aluminum from the fine fraction of shredder ELVs," *Waste Management*, vol. 48, no. 48, pp. 366–373, 2016.

[11] D. Hernandez-Hernandez, T. Larkin, and N. Chouw, "Shake table investigation of nonlinear soil-structure-fluid interaction of a thin-walled storage tank under earthquake load," *Thin-Walled Structures*, vol. 167, Article ID 108143, 2021.

[12] P. Righettini, R. Strada, S. Valilou, and E. KhademOlama, "Nonlinear model of a servo-hydraulic shaking table with dynamic model of effective bulk modulus," *Mechanical Systems and Signal Processing*, vol. 110, no. 110, pp. 248–259, 2018.

[13] M. Iwasaki, K. Ito, M. Kawafuku, H. Hirai, Y. Dozono, and K. Kurosaki, "Disturbance observer-based practical control of shaking tables with nonlinear specimen," *IFAC Proceedings Volumes*, vol. 38, no. 1, pp. 251–256, 2005.

[14] M. N. Nader and A. Astaneh-Asl, "Shaking table tests of rigid, semirigid, and flexible steel frames," *Journal of Structural Engineering*, vol. 122, no. 6, pp. 589–596, 1996.

[15] A. Najafi and B. F. Spencer, "Modified model-based control of shake tables for online acceleration tracking," *Earthquake Engineering & Structural Dynamics*, vol. 49, no. 15, pp. 1721–1737, 2020.

[16] K. Seki, M. Iwasaki, M. Kawafuku, H. Hirai, and K. Yasuda, "Adaptive compensation for reaction force with frequency variation in shaking table systems," *IEEE Transactions on Industrial Electronics*, vol. 56, no. 10, pp. 3864–3871, 2009.

[17] T. L. Trombetti and J. P. Conte, "Shaking table dynamics: results from a test-analysis comparison study," *Journal of Earthquake Engineering*, vol. 6, no. 4, pp. 513–551, 2002.

[18] M. A. Underwood and T. Keller, "Applying coordinate transformations to multi-DOF shaker control," *Sound and Vibration*, vol. 40, no. 1, pp. 14–27, 2006.

[19] V. Hayward, C. Nemri, X. Chen, and B. Duplat, "Kinematic decoupling in mechanisms and application to a passive hand controller design," *Journal of Robotic Systems*, vol. 10, no. 5, pp. 767–790, 1993.

[20] A. Filabi and M. Yaghoobi, "Fuzzy adaptive sliding mode control of 6 DOF parallel manipulator with electromechanical actuators in cartesian space coordinates," *Communications on Advanced Computational Science with Applications*, vol. 2015, no. 1, pp. 1–21, 2015.

[21] G. Yang, "Asymptotic tracking with novel integral robust schemes for mismatched uncertain nonlinear systems," *International Journal of Robust and Nonlinear Control*, vol. 33, no. 3, pp. 1988–2002, 2023.

[22] G. Yang, J. Yao, and Z. Dong, "Neuroadaptive learning algorithm for constrained nonlinear systems with disturbance rejection," *International Journal of Robust and Nonlinear Control*, vol. 32, no. 10, pp. 6127–6147, 2022.

[23] A. R. Plummer and N. D. Vaughan, "Decoupling pole-placement control, with application to a multi-channel electro-hydraulic servosystem," *Control Engineering Practice*, vol. 5, no. 3, pp. 313–323, 1997.

[24] S. K. Jeong and S. S. You, "Precise position synchronous control of multi-axis servo system," *Mechatronics*, vol. 18, no. 3, pp. 129–140, 2008.

[25] C. S. Chen and L. Y. Chen, "Cross-coupling position command shaping control in a multi-axis motion system," *Mechatronics*, vol. 21, no. 3, pp. 625–632, 2011.
[26] C. Adam, "Dynamics of elastic–plastic shear frames with secondary structures: shake table and numerical studies," *Earthquake Engineering & Structural Dynamics*, vol. 30, no. 2, pp. 257–277, 2001.
[27] M. Cao and M. Khan, "Effectiveness of multiscale hybrid fiber reinforced cementitious composites under single degree of freedom hydraulic shaking table," *Structural Concrete*, vol. 22, no. 1, pp. 535–549, 2021.
[28] S. E. Kim, D. H. Lee, and C. Ngo-Huu, "Shaking table tests of a two-story unbraced steel frame," *Journal of Constructional Steel Research*, vol. 63, no. 3, pp. 412–421, 2007.
[29] A. Ashasi-Sorkhabi, H. Malekghasemi, A. Ghaemmaghami, and O. Mercan, "Experimental investigations of tuned liquid damper-structure interactions in resonance considering multiple parameters," *Journal of Sound and Vibration*, vol. 388, no. 3, pp. 141–153, 2017.
[30] A. R. Pandit and K. C. Biswal, "Seismic control of structures using sloped bottom tuned liquid damper," *International Journal of Structural Stability and Dynamics*, vol. 19, no. 09, Article ID 1950096, 2019.
[31] S. Cetin and A. V. Akkaya, "Simulation and hybrid fuzzy-PID control for positioning of a hydraulic system," *Nonlinear Dynamics*, vol. 61, no. 3, pp. 465–476, 2010.
[32] Y. Tagawa and K. Kajiwara, "Controller development for the E-Defense shaking table," *Proceedings of the Institution of Mechanical Engineers-Part I: Journal of Systems & Control Engineering*, vol. 221, no. 2, pp. 171–181, 2007.
[33] D. P. Stoten and N. Shimizu, "The feedforward minimal control synthesis algorithm and its application to the control of shaking-tables," *Proceedings of the Institution of Mechanical Engineers-Part I: Journal of Systems & Control Engineering*, vol. 221, no. 3, pp. 423–444, 2007.
[34] N. Ogawa, K. Ohtani, T. Katayama, and H. Shibata, "Construction of a three–dimensional, large–scale shaking table and development of core technology," *Philosophical Transactions of the Royal Society of London,Series A: Mathematical, Physical and Engineering Sciences*, vol. 359, no. 1786, pp. 1725–1751, 2001.
[35] M. Zeitz, "The extended Luenberger observer for nonlinear systems," *Systems & Control Letters*, vol. 9, no. 2, pp. 149–156, 1987.
[36] Z. Boulghasoul, Z. Kandoussi, A. Elbacha, and A. Tajer, "Fuzzy improvement on Luenberger observer based induction motor parameters estimation for high performances sensorless drive," *Journal of Electrical Engineering & Technology*, vol. 15, no. 5, pp. 2179–2197, 2020.
[37] D. Das, S. Madichetty, B. Singh, and S. Mishra, "Luenberger observer based current estimated boost converter for PV maximum power extraction—a current sensorless approach," *IEEE Journal of Photovoltaics*, vol. 9, no. 1, pp. 278–286, 2019.
[38] F. L. Lewis, D. Vrabie, and V. L. Syrmos, *Optimal Control*, John Wiley & Sons, Hoboken, NJ, USA, 2012.
[39] A. Akers, M. Gassman, and R. Smith, *Hydraulic Power System Analysis*, CRC Press, Boca Raton, FL, USA, 2006.
[40] A. C. Mahato and S. K. Ghoshal, "Energy-saving strategies on power hydraulic system: an overview," *Proceedings of the Institution of Mechanical Engineers-Part I: Journal of Systems & Control Engineering*, vol. 235, no. 2, pp. 147–169, 2021.
[41] Z. M. Wang and S. K. Tan, "Vibration and pressure fluctuation in a flexible hydraulic power systemon an aircraft," *Computers & Fluids*, vol. 27, no. 1, pp. 1–9, 1998.
[42] H. Angue Mintsa, R. Venugopal, J. P. Kenne, and C. Belleau, "Feedback linearization-based position control of an electrohydraulic servo system with supply pressure uncertainty," *IEEE Transactions on Control Systems Technology*, vol. 20, no. 4, pp. 1092–1099, 2012.
[43] O. Cerman and P. Hušek, "Adaptive fuzzy sliding mode control for electro-hydraulic servo mechanism," *Expert Systems with Applications*, vol. 39, no. 11, Article ID 10269, 2012.